

**SPATIAL DISTRIBUTION OF VOLCANIC HOTSPOTS AND PATERAE ON IO: IMPLICATIONS FOR TIDAL HEATING MODELS AND MAGMATIC PATHWAYS.** C. W. Hamilton<sup>1</sup>, C. D. Beggan<sup>2</sup>, R. Lopes<sup>3</sup>, D. A. Williams<sup>4</sup>, and J. Radebaugh<sup>5</sup>, <sup>1</sup>Planetary Geodynamics Laboratory, NASA Goddard Space Flight Center, Greenbelt, MD, 20771, USA, hamilton@dal.ca, <sup>2</sup>British Geological Survey, Edinburgh, UK, <sup>3</sup>Jet Propulsion Laboratory/Caltech, Pasadena, USA, <sup>4</sup>School of Earth and Space Exploration, Arizona State University, Tempe, USA, <sup>5</sup>Geological Sciences, Brigham Young University, Provo, USA.

**Introduction:** Io, the innermost of Jupiter's Galilean satellites, is the most volcanically active body in the Solar System. Io's global mean heat flow is  $\sim 2 \text{ W m}^{-2}$  [1], which is  $\sim 20$  times larger than on Earth. High surface temperatures concentrate within "hotspots" and, to date, 172 Ionian hotspots have been identified by spacecraft and Earth-based telescopes [2]. The Laplace resonance between Io, Europa, and Ganymede maintains these satellites in noncircular orbits and causes displacement of their tidal bulges as the overhead position of Jupiter changes for each moon [3, 4]. Gravitational interactions between Jupiter and Io dominate the orbital evolution of the Laplacian system and generate enormous heat within Io as tidal energy is dissipated. If this energy were transferred out of Io at the same rate as it is generated, then the associated surface heat flux would be  $2.24 \pm 0.45 \text{ W m}^{-2}$  [5]. This estimate is in good agreement with observed global heat flow [e.g., 1], but to better constrain tidal dissipation mechanisms and infer how thermal energy is transferred to Io's surface, it is critical to closely examine the spatial distribution of volcanic features.

End-member tidal dissipation models either consider that heating occurs completely in the mantle, or completely in the asthenosphere [6]. Mixed models typically favor one-third mantle and two-thirds asthenosphere heating [7]. Recent models also consider the effects of mantle–asthenosphere boundary permeability and asthenospheric instabilities [4]. Deep-mantle heating models predict maximum surface heat flux near the poles, whereas asthenosphere heating models predict maxima near the equator—particularly in the Sub-Jovian and Anti-Jovian hemispheres, with smaller maxima occurring at orbit tangent longitudes [4]. Previous studies [e.g., 1, 4, 8] have examined the global distribution of Ionian hotspots and patera (i.e., irregular or complex craters with scalloped edges that are generally interpreted to be volcanic calderas [9]), but in this study, we combine a new geospatial analysis technique with an improved hotspot and patera database [2].

**Methodology:** Our geospatial analysis calculates nearest neighbor (NN) distances along great circles projected onto the surface of spheres or ellipsoids that correspond to the geometry of each of the major planetary bodies within the Solar System. In this case, we use an ellipsoidal geometry for Io, with a semi-major axis of 1829.7 km and semi-minor axis of 1819.2 km.

Our program estimates the expected mean NN distance for a given sample-size and region. The ratio ( $R$ ) between the measured mean NN distance ( $r_a$ ) and expected mean NN distance ( $r_e$ ) is used in combination with the standard deviations of  $r_e$  to assess if the inputs are consistent with the an expected distribution model ( $r_a = r_e$ ), clustered with respect to the model ( $r_a \ll r_e$ ), or repelled relative to the model ( $r_a \gg r_e$ ). A second test statistic,  $c$ , evaluates the significance of the result implied by  $R$ . To calculate  $c$ , the difference between  $r_a$  and  $r_e$  is divided by the expected standard error [10, 11]. A variety of expected models of spatial organization can be tested, but we focus on Poisson (i.e., random) distributions. For a given population size and region, if  $c$  is in its  $\pm 2\sigma$  limits and  $R$  is in its  $\pm 2\sigma$  limits, then the input distribution fits the expected model, whereas if  $c$  and  $R$  are outside their respective  $\pm 2\sigma$  limits, then the input distribution exhibits a significant departure from the model. In such cases,  $R$  can either be less than  $-2\sigma$ , implying smaller than expected (i.e., clustered) NN distances, or  $R$  can be greater than  $+2\sigma$ , implying that the NN distances are greater than expected (i.e., repelled). If  $c$  is in its  $\pm 2\sigma$  limits and  $R$  outside its  $\pm 2\sigma$  limits, or  $c$  is outside its  $\pm 2\sigma$  limits and  $R$  in its  $\pm 2\sigma$  limits, then the results are not significant at the  $2\sigma$  level. We apply this NN technique to 172 hotspots and 529 paterae on Io [2] to examine global and hemispheric distributions of volcanic features in each of the following domains: (1) Global, (2) Sub-Jovian hemisphere, (3) Anti-Jovian hemisphere, (4) Leading hemisphere, (5) Trailing hemisphere, (6) Northern hemisphere, and (7) Southern hemisphere. This allows us to test tidal dissipation models by determining if volcanic features on Io are randomly distributed, or if they exhibit predicted patterns of spatial organization that are related to magmatic upwelling.

**Results:** Hotspots and paterae have modal NN distances of 200–300 km and  $< 50$  km, respectively. Results for  $R$  (Fig. 1) and  $c$  (Fig. 2) show that the global distribution of hotspots, and hotspots in each of the six hemispheres, have NN distributions that are consistent with Poisson (i.e., random) models within  $1\sigma$  thresholds of significance in  $R$  and  $c$  (n.b., a fit within  $\pm 1\sigma$  implies a stronger fit than one within  $\pm 2\sigma$  thresholds). In contrast, paterae have NN distances that are clustered relative to a Poisson model.

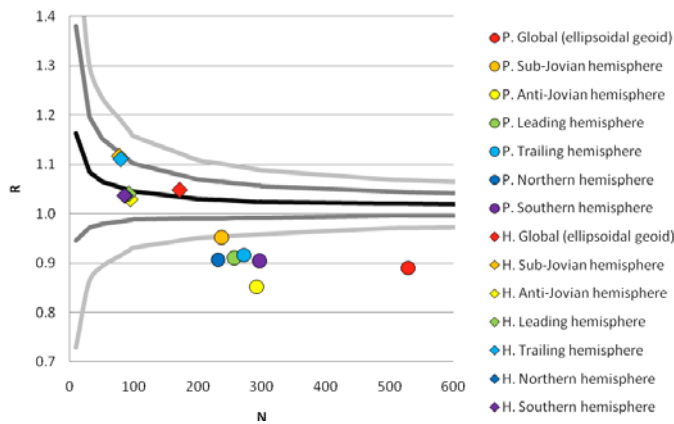


**Figure 1.**  $R$ -values of paterae (P.) and hotspots (H.) on Io. In Figs. 1 and 2, the black lines show ideal values for  $R$  and  $c$ , respectively, given a range of sample-sizes, whereas the dark grey and light grey lines show the  $\pm 1\sigma$  and  $\pm 2\sigma$  thresholds.

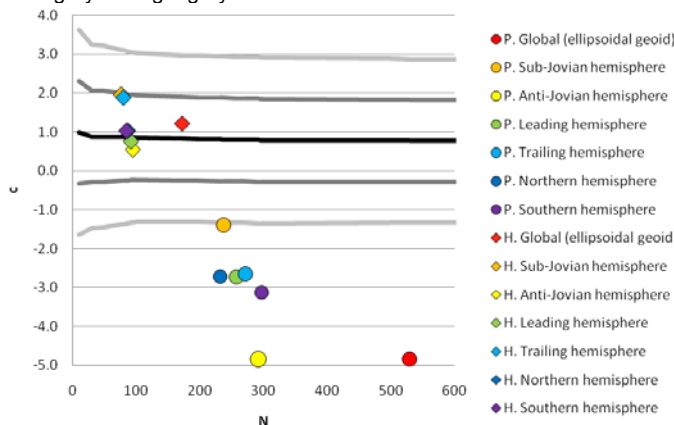


**Figure 2.**  $c$ -values of paterae (P.) and hotspots (H.) on Io. To fit the model of a Poisson NN distribution both  $R$ - and  $c$ -values must be within their respective  $\pm 2\sigma$  limits.

Unlike hotspots, paterae exhibit non-random distributions that are significant beyond  $2\sigma$  thresholds for  $R$  and  $c$  in all regions, except for the Sub-Jovian hemisphere. In the Sub-Jovian hemisphere, paterae have NN distances that are described by a Poisson model within 1 and  $2\sigma$  thresholds of significance in  $R$  and  $c$ .

**Discussion:** Observations from Voyager and Galileo have been used to show that Ionian hotspots appear to have a "uniform" distribution that is not consistent with mantle dominated heating models [1, 8]. However, we caution that these previous studies used "uniform" to describe a uniform random process, rather than a uniform distribution in the sense used by [11]. According to [11], a uniform distribution would imply strong repelling because all points would exhibit equal NN separations. This is not what was meant by [1, 8], who instead used the word "uniform" to mean "Poisson". Our results show that globally, and within all hemispheric domains, hotspot locations are consistent with Poisson distribution models. This agrees with [1,

8] and supports tidal dissipation models involving asthenosphere or asthenosphere-dominated heating [e.g., 4, 12], but not mantle-dominated heating models that would give rise to polar clustering of hotspots.

**Interpretation:** Hotspots provide evidence of current volcanic activity, whereas paterae include volcanic surface features formed over longer periods of geologic history. Given that hotspot locations are consistent with Poisson distribution models, and paterae show pronounced clustering, hotspots may be fed by randomly distributed magmatic upwelling zones, typically separated by 200–300 km, whereas paterae clusters could form over longer timescales as upwelling magma pathways branch out over lateral distances  $< 50$  km.

Spherical harmonic analysis of the global distribution of mountains and volcanic centers on Io [13] shows statistically significant power at degree 2 with anti-correlations between mountains and volcanic centers. The correlations between mountains and volcanic center distributions at high spectral degree could be related to structural links between some mountain blocks and magmatic systems, whereas the anti-correlation at low degree implies that most volcanic features form independently of the mountains. The independent formation of volcanic centers is consistent with our observation that mean NN distances between hotspots appear random. However, structural controls in the vicinity of magma upwelling zones could explain clustering of paterae into preferred volcanic subdomains over longer timescales. Global geologic mapping supports the theory that hotspots concentrate within patera-forming regions [14].

**Conclusions:** Nearest neighbor (NN) analysis shows that Ionian hotspot distributions are consistent with Poisson (i.e., random) models, whereas paterae generally appear clustered relative to Poisson distributions. These results support asthenospheric, or dominantly asthenospheric heating models, and suggest that while locations of active volcanism (i.e., hotspots) appear randomly distributed, patera regions may develop clustering as upwelling magma pathways branch out at shallow depths to feed new volcanic centers.

**References:** [1] Spencer J. R. et al. (2000) *Science*, 288. (1997) *JGR*, 90. [2] Lopes and Spencer (2007) *Io after Galileo*, Praxis-Springer. [3] Peale S. J. (1999) *Ann. Rev. Astron. Astrophys.*, 37. [4] Tackley et al. (2001) *Icarus*, 149. [5] Lainey V. et al. (2009) *Nature*, 459. [6] Schubert G. (1985) *Icarus*, 64. [7] Ross M. N. et al. (1990) *Icarus*, 85 [8] Lopes-Gautier R. et al. (1999) *Icarus*, 140. [9] Radebaugh J. (2001) *JGR*, 106. [10] Beggan C. D. and Hamilton C. W. (2010) *Computers & Geosciences*, 36. [11] Clark P. J and Evans F. C. (1954) *Ecology*, 35. [12] Ross M. N. et al. (1999) *Icarus*, 85. [13] Kirchoff M. R. et al. (2010), *EPSL*, in press, [14] Williams D. A. (2010), *Icarus*, in review.